

Lipotoxicity induced pancreatic beta cell damage is associated with GPR119/MST1/FoxO1 Pathway

Type

Research paper

Keywords

Apoptosis, pancreas, lipotoxicity, FOXO1, GPR119, MST1, Pdx1

Abstract

Introduction

G-protein-coupled receptor 119 (GPR119) is emerging as a potential therapeutic target against type 2 diabetes with beneficial effects on glucose homeostasis. However, the function of GPR119 in lipotoxicity induced pancreatic beta cell apoptosis and the molecular mechanism remains largely unknown.

Material and methods

Impact of GPR119 on pancreatic islet beta cell apoptosis was evaluated in INS-1 cells treated with palmitate. The subsequent modulation of the MST1-FOXO1-Pdx1 signaling pathway and pro-apoptotic caspase-3 system were determined by measuring the target protein and mRNA expression. Dyslipidemia mice with gain and loss of GPR119 function by the application of specific lenti-viral vector was utilized to evaluate the impact of GPR119 on pancreas function in vivo. Lipid metabolism, glucose and insulin response, morphological changes as well as activation/inhibition of MST1-FOXO1-Pdx1 signaling pathway in pancreas were analyzed systematically.

Results

Palmitate treatment stimulated pro-apoptotic response in INS-1 cells, accompanied by inhibition of GPR119 expression and the subsequent activation of the MST1-FOXO1 combined with inhibition of Pdx1 signaling cascade. Activation of GPR119 by MBX prevents INS-1 cell from lipotoxicity induced apoptosis by targeting the MST1-FOXO1-Pdx1 pathway. Moreover, overexpression of GPR119 significantly attenuates the dyslipidemia and dysfunction of the pancreas. In contrast, inactivation of GPR119 by lentiviral vector in mice results in accelerated pancreas apoptosis and malfunction. The protective effects of GPR119 on lipotoxicity induced pancreas dysfunction are associated with modulating the MST1-FOXO1-Pdx1 signaling cascade.

Conclusions

GPR119 alleviates lipotoxicity induced pancreatic beta cell apoptosis and malfunction through regulating MST1-FOXO1-Pdx1 signaling pathway.

1 **Lipotoxicity induced pancreatic beta cell damage is associated with**
2 **GPR119/MST1/FoxO1 Pathway**

3
4
5 **Abstract**

6 **Introduction:** G protein-coupled receptor 119 (GPR119) is a potential therapeutic target for
7 type 2 diabetes (T2D) with beneficial effects on glucose homeostasis. However, the function
8 and molecular mechanism of GPR119 in lipotoxicity induced pancreatic beta cell apoptosis
9 remain undetermined.

10 **Material and methods:** Effect of GPR119 on pancreatic islet beta cell apoptosis was evaluated
11 in INS-1 cells treated with palmitate. The subsequent modulation of the MST1-FOXO1-Pdx1
12 signaling pathway and cell apoptosis were determined. Dyslipidemia mice with overexpression
13 or knockdown GPR119 were utilized to evaluate the impact of GPR119 on pancreas function
14 *in vivo*. Lipid metabolism, glucose and insulin response, morphological changes as well as
15 activation/inhibition of MST1-FOXO1-Pdx1 signaling pathway in pancreas were analyzed
16 systematically.

17 **Results:** Palmitate treatment stimulated pro-apoptotic response in INS-1 cells, accompanied by
18 inhibition of GPR119 expression, activation of the MST1-FOXO1 pathway and inhibition of
19 Pdx1 signaling cascade. Activation of GPR119 by MBX treatment prevented INS-1 cells from
20 lipotoxicity induced apoptosis by targeting the MST1-FOXO1-Pdx1 pathway. Moreover,
21 overexpression of GPR119 significantly attenuated dyslipidemia and dysfunction of the
22 pancreas. In contrast, inactivation of GPR119 in mice resulted in accelerated pancreas apoptosis
23 and malfunction. The protective effects of GPR119 on lipotoxicity induced pancreas
24 dysfunction were associated with modulating the MST1-FOXO1-Pdx1 signaling pathway.

25 **Conclusions:** GPR119 alleviated lipotoxicity induced pancreatic beta cell apoptosis and
26 malfunction through regulating MST1-FOXO1-Pdx1 signaling pathway.

27 **Key words:** lipotoxicity, apoptosis, GPR119, MST1, FOXO1, Pdx1 pancreas.

28

29 **Introduction:**

30 The dysfunction of pancreatic beta cells is the major cause of type 2 diabetes (T2D) and its
31 complications [1-3]. Lipotoxicity, frequently results from prolonged exposure to the free fatty
32 acids (FFA) such as palmitate, impairs the secretion capacity of insulin and induces apoptosis
33 in beta cell [4,5]. Elevated plasma FFAs levels are observed in obesity and type 2 diabetes, with
34 subsequent lipid accumulation and insulin resistance in target tissues [6]. A series of G protein-
35 coupled receptors (GPCR), including GPR119, GPR40, GPR41, GPR43, GPR84 and GPR120,
36 have been identified as FFA specific receptors [7]. FFAs exert different effects on insulin
37 secretion from beta cells. Acute exposure to FFAs stimulates insulin secretion, whereas chronic
38 exposure impairs insulin secretion and increase pancreatic beta cell apoptosis. The dual and
39 opposing effects of FFAs on insulin secretion indicate that FFAs might contribute to both
40 hyper- and hypo-insulinemia during the development of T2D. Therefore, GPCRs which
41 recognize fatty acids and activate the intracellular signaling cascades are of particular important
42 in the treatment of T2D [8].

43 GPR119 is a orphanized G protein-coupled receptor that is predominantly expressed in
44 pancreatic islets [9] and enteroendocrine cells of the gastrointestinal tract [10]. In pancreatic
45 islets, GPR119 is specifically distributed in beta cells and pancreatic polypeptide cells [11].
46 GPR119 can be activated by a variety of endogenous ligands, such as oleoylethanolamide,
47 lysophosphatidylcholine and palmitoylethanolamine [12]. The activation of GPR119 stimulates
48 cAMP and Ca²⁺ release in pancreatic beta cells, enhancing glucose-dependent insulin secretion,
49 thereby decreasing blood glucose in diabetic mice [13,14].

50 Recently, mammalian STE20 like protein kinase 1 (MST1), also called serine/threonine protein
51 kinase 4, has been identified as an essential regulator for pancreatic beta cell differentiation,
52 proliferation, and apoptosis [15]. MST1 is a core component of the hippo signaling pathway,
53 which can be triggered by a variety of apoptotic stimuli, including oxidative stress, Fas ligand,
54 TNF- α , and genotoxic drugs. MST1 is a target and activator of caspases to amplify the apoptotic

55 signaling pathway. MST1 promotes cell death through the regulation of multiple downstream
56 targets such as histone H₂B and members of the FOXO family (Forkhead box O) [16].

57 MST1-FOXO1 signaling pathway is associated with cellular oxidative stress and neuronal
58 apoptosis [17,18]. FOXO1 is mainly expressed in hepatocytes, adipocytes, pancreatic beta
59 cells and vascular endothelial cells. FOXO1 directly involves in regulation of physiological
60 activities such as cell oxidative stress, proliferation, and apoptosis. FOXO1 is closely related to
61 T2D and cardiovascular disease [19]. It has been reported that activated MST1 results in
62 phosphorylation of FOXO1 Ser (212) and promotes apoptosis [20]. Meanwhile, pancreatic beta
63 cell specific FOXO1 transgenic mice were able to maintain beta cell function by increasing the
64 number of beta cells, glucose tolerance and antioxidant capacity. The expression of FOXO1
65 mRNA in islet cells of T2D patients was significantly higher than that in non-diabetic controls
66 subjects [2].

67 The synergistic effect of MST1 and FOXO1 has been proved to play an essential regulatory
68 role in lipid metabolism [21]. Previous study has demonstrated that a high concentration of
69 glucose or fatty acids can cause FOXO1 redistribution in pancreatic beta nuclei [22]. The
70 activation of MST1 can lead to the phosphorylation of FOXO1 and Caspase-3 cleavage [21],
71 indicating that the transcription factor FOXO1 is related to the apoptosis of islet beta cells.
72 However, the specific regulation mechanism still needs further elucidation.

73 The transcription factor pancreatic duodenal homeobox factor 1 (Pdx1) plays a crucial role in
74 pancreatic development and mature pancreatic beta cell function [23]. Downregulation of
75 Pdx1 expression affects insulin production and secretion, and induce beta cells apoptosis
76 [24,25]. Recent studies indicated that MST1 and FOXO1 signaling molecules can regulate pdx1
77 in pancreatic beta cells [26,27]. In this study, we aimed to elucidate the molecular mechanism
78 of GPR119 in lipotoxicity induced beta cell malfunction. A novel signaling cascade of
79 GPR119/FOXO1/Pdx1 in lipotoxicity induced islet cell apoptosis was identified in both *in vitro*
80 and *in vivo*. Our findings extended the current understanding of the molecular mechanism of
81 pancreatic beta cell apoptosis, which provided guidance for the development of new diagnostic
82 and therapeutic drugs against T2D and obesity.

83

84 **Results**

85 **FFA activated the phosphorylation of MST1 and FOXO1 by inhibiting GPR119.**

86 To evaluate the effect of FFA on INS-1 cells, INS-1 cells were stimulated with palmitate. As
87 shown in Figure 1A and 1B, palmitate treatment induced Caspase-3 cleavage in a time-
88 dependent manner and cell apoptosis. Interestingly, GPR119 agonist MBX inhibited MST1
89 phosphorylation and expression, caspase-3 cleavage level (Figure 1C), and attenuated the
90 palmitate-induced INS-1 cell apoptosis and (Figure 1D). Further gene expression analysis
91 revealed that MBX treatment decreased Bax mRNA levels while stimulated Pdx1 and Insulin
92 mRNA expression (Figure 1E). Lipid analysis showed that cellular content of TG and FFA
93 content was significantly decreased in INS-1 cells treated with MBX (Figure 1F and 1G)
94 (P<0.05). Insulin levels from INS-1 cells was also significantly increased after MBX
95 intervention (Figure 1H). In addition, the intracellular calcium concentration, was significantly
96 increased in MBX treated INS-1 cells (Figure 1D).

97 To investigate effect of MST1 on possible downstream signaling cascade FOXO1 and Pdx1,
98 INS-1 cells was overexpressed or knocked down MIST. As shown in Figure 2A and 2B, MST1
99 overexpression stimulated FOXO1 phosphorylation and activation of caspase-3 in palmitate-
100 treated INS-1 cells. As expected, Pdx1 which is negatively regulated by MST1 was
101 downregulated. Therefore, MST1 overexpression alleviated palmitate induced INS-1 cell injury.
102 In contrast, knock down of MST1 resulted in inactivation of the MST1-FOXO1 signaling
103 pathway while upregulation of Pdx1 expression. These findings indicated that FOXO1 and
104 Pdx1 are downstream molecules of MST1 signaling in islet cells.

105

106 **Calmodulin (CaM) inhibitor CPZ activated MST1-FOXO1 signaling pathway.**

107 Previous study demonstrated that treatment of CaM antagonist CPZ in pancreatic cells affects
108 the secretion of insulin by inhibition of Ca²⁺ influx [28]. In the current study, increased calcium
109 concentration was also observed in palmitate treated INS-1 cells with GPR119 activation

110 (Figure 1I), accompanied by increased insulin levels. Therefore, the potential involvement of
111 CaM in palmitate induced signaling alterations was evaluated in CPZ treated INS-1 cells. As
112 shown in Figure 3A and 3B, intervention of CaM in palmitate treated INS-1 cells increased the
113 phosphorylation of MST1 and FOXO1, cMST1, activated the apoptotic protein Caspase-3.
114 These results indicated that palmitate induced MST1-FOXO1 signaling pathway was mediated
115 through the Ca²⁺ and Calmodulin messenger systems (Figure 3).

116

117 **Overexpression of GPR119 alleviated pancreatic injury in C57BL/6J mice induced by** 118 **high-fat diet.**

119 After 18 weeks intervention, mice in high-fat diet (HFD) group showed significantly higher
120 body weight gain compared with mice in the low-fat diet (LFD) group (Figure 4A). In response
121 to a bolus of glucose injection, analysis of area under curve indicated that mice in HFD group
122 demonstrated significant glucose intolerance compared with mice in LFD group (Figure 4B).
123 Similarly, in response to a bolus of insulin administration, a slower decrease in blood glucose
124 was observed in HFD group compared with the LFD group, indicating insulin intolerance in
125 these HFD feeding mice (Figure 4C). The GPR119 overexpression mice showed improved lipid
126 and glucose homeostasis (Table 1). Immunohistochemical staining showed that the number of
127 brown granules in GPR119 overexpression group was higher than that in the control group
128 (Figure 4D). Besides, a substantial decrease in pancreatic islet cell amount was observed in
129 GPR119 shRNA mice compared with those in GPR119 overexpression group (Figure 4E).

130 The pathomorphological changes in pancreatic tissues were examined by electron microscopy.
131 More severe damage was observed in pancreatic islet cells in HFD group compared to the LFD
132 group (Figure 5A). The expression of GPR119 also impacted the ultrastructure of pancreatic
133 beta cells. More severe damage was detected in the HFD + GPR119 shRNA group than that in
134 GPR119 overexpression group. The pancreatic cell damage was characterized by irregular cell
135 morphology, nuclear condensation, nuclear chromatin condensation, mitochondria swollen,
136 and a large number of fat droplets with smaller electron density, in which the insulin-secreting

137 particles in the islet cells were reduced (Figure 5B). The results of morphological experiments
138 indicated that GPR119 could protect pancreatic beta cells from damage in response to excess
139 lipid (Figure 5C).

140 The impact of GPR119 on pancreatic signaling cascade was evaluated by determination of the
141 target protein expression. As indicated in Figure 6, HFD induced down-regulation of GPR119
142 and activation of MST1-FOXO1 signaling. In consistent with results in INS-1 cells, GPR119
143 overexpression in mice resulted in inhibition of pancreatic MST1 and FOXO1 activation,
144 reflecting by decreased cMST1, phosphorylated MST1, phosphorylated FOXO1, and cleaved
145 caspase-3.

146

147 Discussion

148 Previous studies demonstrated that activation of GPR119 by its specific agonists enhances
149 intracellular cAMP and GSIS release, and stimulates the secretion of GLP-1 and GIP, and has
150 a certain inhibitory effect on the apoptosis of pancreatic beta cells [29,30]. Our study extended
151 the current understanding of the function of GRP119 in islet cell by identifying the novel
152 downstream MST1-FOXO1-Pdx1 signaling cascade. In palmitate induced lipotoxic INS-1 cell
153 model, MBX mediated GPR119 activation notably reduced islet cell apoptosis rate compared
154 with the control group, accompanied by inhibition of MST1 and FOXO1 activation, decreased
155 Pdx1 expression and caspase-3 cleavage. Subsequent *in vivo* studies further confirmed that
156 regulation of beta cell apoptosis by GPR119 was directly associated with the
157 MST1/FOXO1/Pdx1 cascade. The GPR119 activation plays an important regulatory role in the
158 survival and function of pancreatic cells through the interaction of MST1-FOXO1-Pdx1. In
159 consistence with previous studies, our results demonstrated that MST1-FOXO1 signaling
160 pathway plays an important role in the process of neuronal apoptosis.

161 Activation of GPR119 has previously been proven to directly stimulate pancreatic beta cell
162 insulin release and enterocytes incretins secretion [31]. In pancreatic beta cells, insulin secretion
163 is initiated by rapid increase of intracellular Ca²⁺ concentration [32], which is regulated by

164 Calmodulin (CaM). In accordance with these studies, inhibition of the binding of Ca²⁺ to CaM
165 by CPZ in INS-1 cells activated the apoptosis signaling pathway in response to FFA stimulation,
166 accompanied by activated MST1-FOXO1 signaling cascade and down-regulation of Pdx1
167 expression. These findings indicated that GRP119 might function through Ca²⁺ to CaM
168 pathway in islet cells. However, the direct interaction of GRP119 and the calcium pathway still
169 needs further verification in the future studies.

170 More recently, MST1-FOXO1 pathway and endoplasmic reticulum (ER) stress have been
171 identified to be involved in the pancreatic beta cells malfunction and apoptosis [33,34]. MST1
172 in pancreas beta cells can be activated by proinflammatory cytokines as well as glucotoxicity
173 and lipotoxicity [35]. MST1 activation enhanced the impairment of pancreatic beta cells by
174 stimulating phosphorylation of stress kinase JNK, apoptotic mediator caspase-3 and intrinsic
175 cell death mediator BIM, and meanwhile inhibiting the predominant pro-survival AKT
176 signaling cascade [36-38]. In addition, the activation of Pdx1, a vital regulator for insulin
177 secretion and beta cell survival through interaction with GLUT-2 and glucokinase, was also
178 inhibited once MST1 activation.

179 Lipotoxicity activated the MST1 phosphorylation and the downstream signaling cascades such
180 as FOXO1, caspase-3 and Pdx1. MST1 was essential for the downstream signaling pathways
181 associated with beta cell apoptosis and malfunction in response to lipotoxicity. In
182 hyperlipidemia mouse models, the activation of the MST1 signaling in the pancreas was
183 correlated with impaired glucose and insulin metabolism, reflected with glucose intolerance,
184 and decreased insulin levels.

185 Our study extended the current understanding of FFA-MST1-FOXO1-Pdx1-beta cell
186 malfunction pathway by revealing GRP119 as an essential upstream modulator. In our model,
187 lipid loading in INS-1 cells decreased GPR119 expression, which subsequently activated the
188 MST1 signaling pathway. The cleaved MST1 stimulated the caspase-3 cleavage and FOXO1
189 phosphorylation as well as inhibited Pdx1 expression, resulting in the acceleration of beta cell
190 death and impaired insulin secretion. The GRP119 modulation might be mediated through the
191 secondary messenger Ca²⁺ and CaM systems.

192 The impact of GPR119 in the pancreases function was further confirmed in the hyperlipidemia
193 mouse model. After 18 weeks of high-fat feeding, mice developed obesity, insulin resistance,
194 glucose intolerance, and hyperlipidemia. Interestingly, overexpression of GPR119 in these
195 hyperlipidemia mice resulted in a significant decrease in TG, TC and FFA, and a substantial
196 increase in the content of insulin and C peptide compared to the control mice. Importantly,
197 GPR119 overexpression also significantly alleviated hyperlipidemia induced islet damage and
198 apoptosis, featured by the chromatin condensation, mitochondria swelling and deformation, and
199 decreased cytoplasmic endocrine granules. The protective effects of GPR119 against pancreas
200 cell apoptosis in mice were associated with modulation of dysfunctional MST1-FOXO1-Pdx1
201 signaling cascade induced by prolonged fatty acids exposure.

202 In summary, the current study demonstrated that activation of GPR119 substantially attenuated
203 lipotoxicity induced pancreatic beta cell damage. The effects of GPR119 was associated with
204 Ca^{2+} - calmodulin pathway and the subsequent modulation of MST1-FoxO1-Pdx1 signaling
205 cascade, which affected pancreatic beta cell function and apoptosis, and finally impacted the
206 insulin secretion and glucose metabolism. This study provided an experimental basis for
207 understanding the mechanism of GPR119 in high-fat induced pancreatic beta cell dysfunction,
208 laying the foundation for the study of the mechanism of obesity and pancreatic beta cell damage
209 and malfunction.

210

211 **Methods**

212 **Cell culture.**

213 INS-1 cells (SCC207, EMD Millipore, Burlington, MA, USA) were cultured in RPMI 1640
214 medium supplemented with 10% fetal bovine serum (FBS; Gibco), 50 IU/mL penicillin, 50
215 mg/L streptomycin, 10 mM HEPES, 2 mM L-glutamine, 1 mM sodium pyruvate and 50 μ M
216 beta-mercaptoethanol. Cells were cultured at 37 °C in a humidified atmosphere with 5% CO₂.
217 For palmitate treatment, INS-1 cells were plated into 12 well plates and cultured for 24 hours,
218 250 μ M PA diluted in fatty acid-free bovine serum albumin (BSA, Sigma-Aldrich, St. Louis,

219 MO, USA) was added to the medium and incubated for indicated time points. BSA was used
220 as vehicle control. In selective studies, following 12 h of PA treatment, INS-1 cells were treated
221 with GPR119 agonist MBX (4 μ M) for 10 minutes or CAM antagonist CPZ (0.5 mM) for 60
222 minutes. For MST1 overexpression and knockdown, INS-1 cells were treated with PA (250.0
223 μ M) for 12 hours and then transfected with MST1 overexpression plasmid or MST1 silencing
224 shRNA plasmid for 72 hours.

225

226 **Plasmid Constructs.**

227 To generate MIST1 overexpression plasmid, full-length rat MST1 was amplified from
228 previously constructed plasmid pMD19-MST1 using the following primers: forward: 5'- GCT
229 GGA TCC GCC ACC ATG GAG ACC GTG CAA CTG AGG AAC-3'; reverse; 5'- ATA GCG
230 GCC GCT CAG AAG TTC TGT TGC CCC TCT TCT TGG C-3'. The amplicon was inserted
231 into the pcDNA3.1 vector with the Not I and *Bam*H I recognition sites. To silence MST1,
232 siRNA against rat MST1 (MST1 siRNA: sense, 5'-GAT CCG CTG GTT CTG TAT CCG ATA
233 TTC TCG AGA ATA TCG GAT ACA GAA CCA GCT TTT G-3', anti-sense, 5'-AAT TCA
234 AAA AGC TGG TTC TGT ATC CGA TAT TCT CGA GAA TAT CGG ATA CAG AAC
235 CAG CG-3') was synthesized (Sangon Biotech, Shanghai, China) and inserted into the
236 pGreenPuro vector. To generate lentiviral transfer plasmids containing GRP119 or shGRP119,
237 mouse GRP119 was amplified from pMD19-GRP119 plasmid using the following primers:
238 forward: 5'-GCT CTA GAG CCG CCA TGG AGT CAT CCT TCT CAT TTG GAG TG-3';
239 reverse; 5'-CGG GAT CCG CCA TCG AGC TCC GGA TGG CT-3'. GRP 119 shRNA was
240 annealed (sense, 5'-GCT AGT TAC CTT CCT GTC AGA GTA ACT AGC CCA GAA ATA
241 GCC TTT TTG-3'; anti-sense, 5'-AAT TCA AAA AGG CTA TTT CTG GGC TAG TTA CTC
242 TGA CAG GAA GGT AAC TAG CCC AGA AAT AGC CG-3'). The amplified GRP119
243 and annealed shGRP119 were inserted into PCDH-CMV-MCS-EF1-GFP and pGreen-CMV-
244 coGFP-T2A-PURO-H1 vectors, respectively. The product was transformed into Stbl3
245 chemically-competent *E.coli* cells, and the plasmids were extracted by Plasmid Midiprep Kit
246 (Qiagen, Germany).

247

248 **Transfection.**

249 To overexpress or silence MST1, INS-1 cells were transfected with overexpression or siRNA
250 plasmids using Lipofectamine 2000 (Invitrogen, Carlsbad, CA, USA) according to the
251 manufacturer's instructions. For lentiviral plasmid transfection, constructed lentiviral transfer
252 plasmid, PLP, PLP2 and PLP/VSVG vectors were transfected into 293T cells using
253 Lipofectamine 2000. At 8 hours post transfection, the 293T cells were switched to complete
254 medium and cultured for 48 hrs. The supernatant was then centrifuged at 4000g at 4°C for 10
255 min to remove cell debris and filtered through a 0.45 um filter membrane.

256

257 **Realtime PCR.**

258 Total RNA was isolated by Trizol (Invitrogen, USA) according to the manufacturer's
259 instructions. The RNA quality was determined by NanoDrop 2000 (Thermo Fisher, USA). The
260 first-strand cDNA was synthesized using First Strand cDNA Synthesis Kit (Invitrogen, USA).
261 Realtime PCR was performed by SYBR Master Mix on the ABI 7500 Realtime PCR system
262 (Applied Biosystems, USA) as previously described [39]. The relative mRNA expression of
263 target genes to endogenous control glyceraldehyde-3-phosphate dehydrogenase (GAPDH) was
264 calculated using the $2^{-\Delta\Delta CT}$ method. The primer sequences were summarized in Table 2.

265

266 **Flow cytometry analysis.**

267 Apoptosis analysis was carried out as previously described [40]. The treated cells were
268 dissociated by trypsin and washed with PBS. Subsequently, cells were stained with annexin V
269 FITC (Bio-Rad, USA) and RaddiDrop propidium iodide (Bio-Rad, USA) in binding buffer for
270 20 mins in the dark. Stained cells were subjected to flow cytometry analysis using the
271 FACSCalibur system (BD Biosciences, USA).

272

273 **Animal experiments.**

274 All animal experiments were performed following the Guide for the Care and Use of Laboratory
275 Animals, and all the animal experimental protocols were approved by the Institutional Animal
276 Care and Use Committee (IACUC) at Ningxia Medical University, Yinchuan, China (approval
277 No. 2019-011). Mice were housed in laboratory animal center of Ningxia Medical University
278 with a 12-hour light/dark cycle. The specific-pathogen-free (SPF) male nude C57BL/6 mice (6
279 week-old; 16 – 19 g; n = 25 for each group) were fed a LFD containing 10% kcal from fat
280 (MD12031, Mediscience, China) or a HFD containing 60% kcal from fat (MD12033,
281 Mediscience, China) for 18 weeks. For overexpression of GPR119 in the pancreas, 1.0×10^8
282 plaque-forming units (PFU) of LV-GFP, LV-GPR119, LV-shctrl and LV-shGPR119 (n = 5 for
283 each subgroup) were injected into HFD-fed or LFD-fed mice via the tail vein.

284

285 **Metabolic measurement.**

286 For the glucose tolerance test (GTT) and insulin tolerance test (ITT), mice were fasted for 4
287 hours and then were injected with 2g/kg D-glucose or 1IU/kg insulin intraperitoneally. Blood
288 glucose levels were measured at 15, 30, 60, and 90 mins post-injection using a glucometer.
289 Mice were euthanized after 19 weeks of animal experiments. Blood was collected from heart
290 puncture, and plasma was further isolated. Plasma Insulin and C peptide levels were determined
291 by ELISA kits (Thermofisher, USA). Plasma total cholesterol, triglycerides, free fatty acids
292 levels were determined by commercial kits (Wako, Japan).

293

294 **Immune-histochemistry.**

295 The pancreas was isolated from experimental mice and fixed with formalin for 48 hours. Briefly,
296 mice were anesthetized with 4% chloral hydrate and transcardially perfused with PBS and 4%
297 paraformaldehyde, subsequently decapitated. Tissues were then embedded with paraffin and
298 the tissue blocks were sliced into 5 μ m paraffin sections. Immunohistochemical staining of

299 tissue section were incubated with 3% H₂O₂ for 10 minutes to inactivate the endogenous
300 peroxidase, followed by incubation with primary antibody GPR119 (1:500, AbCam,
301 Cambridge, UK) for 2 hours and secondary antibody HRP-goat anti-rabbit IgG (1:2,000,
302 Abcam, Cambridge, UK) for 30 minutes at room temperature. Sections were rinsed in cold PBS
303 (5 times, 3 minutes per time), incubated in avidin–biotin complex (Vecta stain Elite ABC Kit,
304 Vector Laboratories) for 1 hour at 20°C and rinsed with PBS (3 times, 10 minutes per time).
305 Finally, sections were developed in diaminobenzidine substrate for 5 minutes at 25°C and
306 counterstained with hematoxylin. The sections were further differentiated in 0.1% HCl,
307 dehydrated in gradient alcohol, cleared by xylene and mounted with resinous media. Images
308 were obtained with microscope under bright field.

309

310 **Western blot.**

311 The protein expression levels were analyzed as previously described [41]. In brief, protein was
312 extracted from INS-1 cells or pancreas tissues using protein lysis buffer (R0010, Solarbio).
313 After centrifugation at 12,000rpm for 30 mins, protein was harvested from supernatant and
314 quantified by bicinchoninic acid (BCA reagents, Thermofisher, USA). 50 µg cell lysates were
315 re-suspended in SDS sample loading buffer, subjected to 10% SDS-PAGE gel and transferred
316 onto a PVDF membrane (Millipore, Bedford, MA, USA). After blocking in Tris-buffered saline
317 with 0.2 % of Tween 20 (TBST) containing 5% w/v non-fat milk for 2 hours at room
318 temperature, membranes were further incubated with specific primary antibodies overnight at
319 4 °C. The following primary antibodies were used: Caspase-3, phospho-MST1/ MST1, Pdx1
320 (Cell Signaling, USA), GRP-119 and β-actin (ab75312, Abcam, USA), phospho-FOXO1 /
321 FoxO1 (Sata Cruz Biotechnology, Dallas, TX, USA), insulin receptor and BAX (Proteintech,
322 Chicago,IL,USA). Following incubation with the specific HRP-conjugated antibody,
323 chemiluminescence signal was detected using ECL (ECL-808-25, Biomiga, USA). The
324 membranes were developed, and immunoblot bands were subjected to relative densitometric
325 analysis. Protein expression was quantified by determining the relative density of target protein
326 band to the internal control band.

327

328 **Statistical analysis.**

329 All results are expressed as the mean \pm SEM. Data between groups was analyzed by one-way
330 or two-way ANOVA, followed by post hoc Tukey's multiple comparison analysis. Differences
331 between groups were considered statistically significant at $P < 0.05$. Analysis was conducted
332 using GraphPad Prism 6 software.

333

334 **Competing interests:**

335 The authors declare that they have no competing interests.

336

337 **Funding**

338 This work was supported by the National Natural Science Foundation of China (No. 81670798),
339 the spring plan of Ministry of Education(Z2016039), West China Top Class Discipline Project
340 in Basic Medical Sciences, Ningxia Medical University.

341

342 **Acknowledgements**

343 The authors would like to thank Dr. Jiajun Zhao for critical comments.

344

345 **Author Contributions**

346 Y.Y. and L.C. designed the study. L.R.M., J.N.L, Y.L.S and Y.H.L conducted the experiments.
347 Y.L., Y.W and H.S. analyzed the data. Y.S.L., H.Q. performed the animal experiments. Y.Y.,
348 L.C. and L.R.M. wrote and edited the manuscript. All authors reviewed and approved the
349 content of the paper.

350

351 **Ethics approval and consent to participate**

352 All animal experiments were performed in accordance with the Guide for the Care and Use of
353 Laboratory Animals, and all the animal experimental protocols were approved by the
354 Institutional Animal Care and Use Committee (IACUC) at Ningxia Medical University
355 (Yinchuan, China).

356

357 **Abbreviations:**

358 GPR119: G-protein-coupled receptor 119; MST1: mammalian STE20 like protein kinase 1;
359 **T2D**: type 2 diabetes; FOXO1 (Forkhead box O1); FFA: free fatty acids; Pdx1: pancreatic
360 duodenal homeobox factor 1; CaM: Calmodulin; CPZ: Chlorpromazine; HFD: high fat diet;
361 LDF: low fat diet; PA: palmitate.

362

363

364 **Figure legends:**

365 **Figure 1. Palmitate treatment stimulated the phosphorylation of MST1 by inhibiting**
366 **GPR119 in INS-1 cells.** (A). INS-1 cells were treated with Palmitate (PA) (250 μ M) at
367 indicated time points. The activated caspase-3 expression (cl-Cas 3) was determined by western
368 blot and quantified by relative density to β -actin. Data are expressed as mean \pm SEM (n = 5). *,
369 $P < 0.05$ vs. control. (B, D) Detection of apoptosis rate by flow cytometry. * $P < 0.05$, PA vs
370 control; PA+MBX vs. control+MBX. (C). INS-1 cells were treated with 250 μ M palmitate for
371 12 h, followed by treatment of 4 μ M MBX for 10 min. The expression of GPR119, MST1,
372 pMST1, cIMST1 and caspase-3 cleavage (clC3) expression were determined by western
373 blotting and quantified by relative density to β -actin. Data are expressed as mean \pm SEM (n =
374 5). *, $P < 0.05$ vs. control. (E) Target mRNA expression in INS-1 cells treated with MBX. Data
375 are expressed as mean \pm SEM (n = 5). (F, G) Effects of GPR119 agonist MBX on cellular TG
376 and FFA contents in INS-1 cells. Data are expressed as the mean \pm SEM (n = 5). (H) Insulin
377 secretion in PA treated INS-1 cells in the presence/absence of MBX at indicated time points.

378 **(I)** Intracellular calcium concentration in INS-1 cells determined by flow cytometry. Data are
379 expressed as the mean \pm SEM (n = 5). **P* < 0.05, #*P* < 0.01 vs. control. Experiments were
380 repeated three times.

381 **Figure 2.** Target protein expression in PA treated INS-1 cells with gain and loss of MST1
382 expression. **(A)** INS-1 cells were treated with PA (250 μ M) for 12 hrs and then were incubated
383 MST1 overexpression plasmid MST1 or MST1 shRNA plasmid for 72 hrs. Protein expression
384 of MST1, pMST1, FOXO1, pFOXO1, cMST1 and caspase-3 cleavage (cC3) was determined
385 by western blot. **(B)** Quantification of protein bands by densitometry analyses. Data are
386 expressed as the mean \pm SEM (n = 5). **P* < 0.05, #*P* < 0.01 vs. control. Experiments were
387 repeated three times.

388 **Figure 3.** Target protein expression in INS-1 cells treated with Palmitate in the presence/
389 absence of CPZ. INS-1 cells were treated with palmitate (250 μ M) for 12 h, followed by
390 treatment of CPZ (0.5 mM) for 60 min. **(A)** The protein levels of MST1, pMST1, FOXO1,
391 pFOXO1, cMST1 and cleaved caspase-3 (cC3) were determined by western blot using
392 specific antibodies. **(B).** Quantification of the protein bands by densitometry and normalized to
393 β -actin. Data are expressed as mean \pm SEM (n = 5). **P* < 0.05, #*P* < 0.01; CPZ treated vs.
394 control. All data were derived from three independent experiments.

395 **Figure 4. Overexpression of GPR119 alleviated pancreatic injury in C57BL/6J mice**
396 **induced by high fat feeding.** 6-week-old male C57 mice were fed on HFD or LFD for 18
397 weeks and then were given either LV-GPR119 or LV-shGPR119 by tail vein injection. **(A).**
398 Body weight of mice on a LFD or HFD. Body weight of the experimental mice were measured
399 weekly and shown as the mean \pm SEM (n = 25). **(B, C).** Glucose tolerance and insulin tolerance
400 test in LFD and HFD mice at 12 weeks feeding. **(D).** GPR119 protein expression in the pancreas
401 of mice determined by IHC (400 X). **(E).** Pancreas tissue morphological changes were
402 determined by HE staining. Representative images (400X) are shown. Data are expressed as
403 the mean \pm SEM (n = 5). **P* < 0.05, #*P* < 0.01 vs. control.

404 **Figure 5.** Pancreas damage of mice on a high fat diet. Mice were fed on HFD or LFD for 18
405 weeks and then were given either LV-GPR119 or LV-shGPR119 by tail vein injection for 1

406 week (n=5) (A). Electron microscope images of pancreatic tissue section of LFD/HFD mice.
 407 (B). Electron microscopy images of pancreas tissue on HFD group with GPR119
 408 overexpressing or GPR119 silencing. (a,d X3000; b,e X5000; c,f X15000). (C). Model of
 409 pancreas GRP119 function in pancreas high fat milieu. Lipid loading in INS-1 cells decreased
 410 GPR119 expression which subsequently activated the MST1 signaling. Active cleaved MST1
 411 then stimulated the caspase-3 cleavage and FOXO1 phosphorylation as well as inhibited Pdx1
 412 activation. Such alteration in the signaling cascade resulted in acceleration of beta cell death
 413 and impaired insulin secretion. In response to lipotoxicity, the function of GPR119 is likely
 414 through affecting intracellular $[Ca^{2+}]$ release.

415 **Figure 6.** HFD induced down-regulation of GPR119 and activation of MST1-FOXO1 signaling.
 416 (A) Mice were fed on HFD or LFD for 18 weeks and then were given either LV-GPR119, LV-
 417 GFP, LV-shGPR119 or LV-sh Control by tail vein injection for 1 week. Pancreas was isolated,
 418 and protein was extracted. Protein expression of MST1, pMST1, FOXO1, pFOXO1, cMST1
 419 and caspase-3 cleavage (cC3) was determined by western blot. (B, C) Quantification of protein
 420 bands by densitometry analyses. Data are expressed as the mean \pm SEM (n = 5). * $P < 0.05$, # P
 421 < 0.01 vs. control. Experiments were repeated three times.

422

423 **Table 1.** Detection of insulin, C peptide and FFA in serum of mice.

Group	Insulin (IU/mL)	C peptide (ug/mL)	FFA (mmol/L)
LFD	19.95 \pm 0.09	0.36 \pm 0.03	35 \pm 3.68
LFD-LV+GFP	19.75 \pm 0.37	0.32 \pm 0.02	16 \pm 0.89
LFD-LV+GPR119	14.00 \pm 0.15 ^a	0.27 \pm 0.01 ^a	6 \pm 0.73 ^a
LFD-LV+shCtrl	16.63 \pm 0.39	0.30 \pm 0.007	25 \pm 3.13
LFD-LV+shGPR119	15.63 \pm 0.43	0.35 \pm 0.007	35 \pm 8.02
HFD	23.52 \pm 0.20	0.28 \pm 0.007	55 \pm 10.6
HFD-LV+GFP	17.70 \pm 0.42	0.20 \pm 0.007	15 \pm 1.03
HFD-LV+GPR119	40.1 \pm 0.33 ^c	0.70 \pm 0.007 ^c	5 \pm 0.06 ^c

HFD-LV+shCtrl	31.77±0.46	0.58±0.03	13±1.08
HFD-LV+shGPR119	41.28±0.85	0.57±0.03	11±1.32

424 Remarks: a, LFD-LV+GPR119 vs LFD-LV+GFP, P < 0.05; c, HFD-LV+GPR119 vs HFD-
425 LV+GFP, P < 0.05.

426

427

428 **Table 2.** Primers used for Realtime PCR.

Primer name	Primer Sequence (5'-3')
Bax-F	GGTTGTCGCCCTTTCTA
Bax-R	CGGAGGAAGTCCAATGTC
Bcl2-F	GATGTGATGCCTCTGCGAAG
Bcl2-R	CATGCTGATGTCTCTGGAATCT
Pdx1-F	CCACCCCAGTTTACAAGCTC
Pdx1-R	TGTAGGCAGTACGGGTCCTC
Insulin-F	GCGGGCTGCGTCTAGTTGCAGTAG
Insulin-R	ATGGCCCTGTGGATGCGCCTCCTG
GAPDH-F	GCAAAGACTGAACCCACTAATTT
GAPDH-R	TGCTCTGTTGTTACTTGGAGAT

429

430

431 References

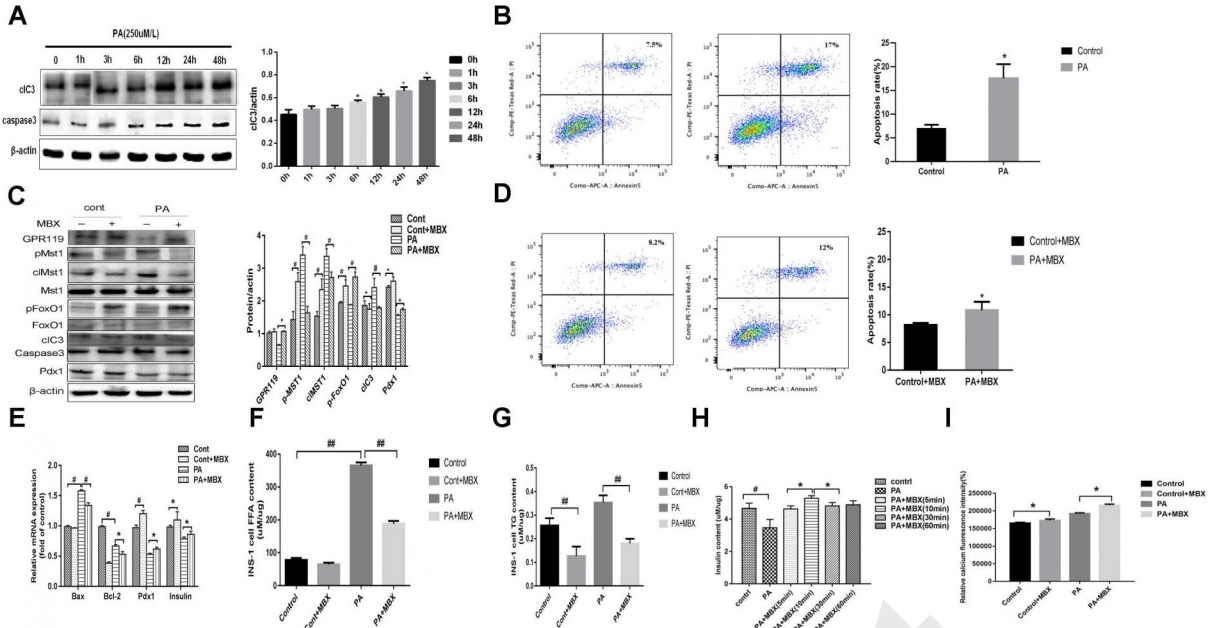
- 432 1. Boden G. Role of fatty acids in the pathogenesis of insulin resistance and NIDDM.
433 Diabetes 1997; 46: 3-10.
- 434 2. Del Guerra S, Lupi R, Marselli L, et al. Functional and molecular defects of pancreatic

- 435 islets in human type 2 diabetes. *Diabetes* 2005; 54: 727-735.
- 436 3. Ying C, Wang S, Lu Y, et al. Glucose fluctuation increased mesangial cell apoptosis
437 related to AKT signal pathway. *Arch Med Sci* 2019; 15: 730-737.
- 438 4. Sharma RB and Alonso LC. Lipotoxicity in the pancreatic beta cell: not just survival
439 and function, but proliferation as well? *Curr Diab Rep* 2014; 14: 492.
- 440 5. Oh YS, Bae GD, Baek DJ, et al. Fatty Acid-Induced Lipotoxicity in Pancreatic Beta-
441 Cells During Development of Type 2 Diabetes. *Front Endocrinol (Lausanne)* 2018; 9:
442 384.
- 443 6. Haber EP, Ximenes HM, Procopio J, et al. Pleiotropic effects of fatty acids on
444 pancreatic beta-cells. *J Cell Physiol* 2003; 194: 1-12.
- 445 7. Reimann F and Gribble FM. G protein-coupled receptors as new therapeutic targets for
446 type 2 diabetes. *Diabetologia* 2016; 59: 229-233.
- 447 8. Piro S, Anello M, Di Pietro C, et al. Chronic exposure to free fatty acids or high glucose
448 induces apoptosis in rat pancreatic islets: possible role of oxidative stress. *Metabolism:
449 clinical and experimental* 2002; 51: 1340-1347.
- 450 9. Soga T, Ohishi T, Matsui T, et al. Lysophosphatidylcholine enhances glucose-
451 dependent insulin secretion via an orphan G-protein-coupled receptor. *Biochem
452 Biophys Res Commun* 2005; 326: 744-751.
- 453 10. Chu ZL, Carroll C, Alfonso J, et al. A role for intestinal endocrine cell-expressed g
454 protein-coupled receptor 119 in glycemic control by enhancing glucagon-like Peptide-
455 1 and glucose-dependent insulinotropic Peptide release. *Endocrinology* 2008; 149:
456 2038-2047.
- 457 11. Ning Y, O'Neill K, Lan H, et al. Endogenous and synthetic agonists of GPR119 differ
458 in signalling pathways and their effects on insulin secretion in MIN6c4 insulinoma
459 cells. *British journal of pharmacology* 2008; 155: 1056-1065.
- 460 12. Moran BM, Abdel-Wahab YH, Flatt PR, et al. Activation of GPR119 by fatty acid
461 agonists augments insulin release from clonal beta-cells and isolated pancreatic islets
462 and improves glucose tolerance in mice. *Biol Chem* 2014; 395: 453-464.
- 463 13. Dhayal S and Morgan NG. The significance of GPR119 agonists as a future treatment
464 for type 2 diabetes. *Drug news & perspectives* 2010; 23: 418-424.
- 465 14. Lauffer LM, Iakoubov R and Brubaker PL. GPR119 is essential for
466 oleoylethanolamide-induced glucagon-like peptide-1 secretion from the intestinal
467 enteroendocrine L-cell. *Diabetes* 2009; 58: 1058-1066.
- 468 15. Ardestani A and Maedler K. MST1: a promising therapeutic target to restore functional
469 beta cell mass in diabetes. *Diabetologia* 2016; 59: 1843-1849.
- 470 16. Bi W, Xiao L, Jia Y, et al. c-Jun N-terminal kinase enhances MST1-mediated pro-

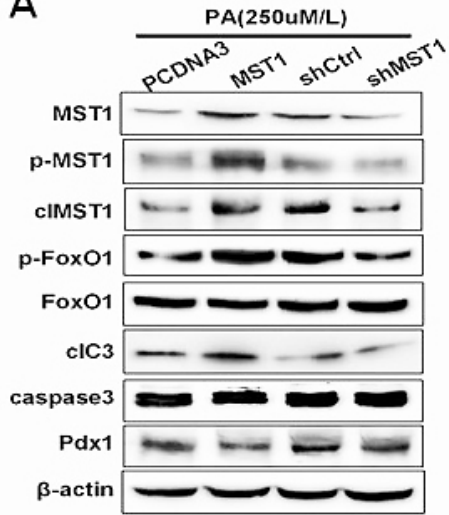
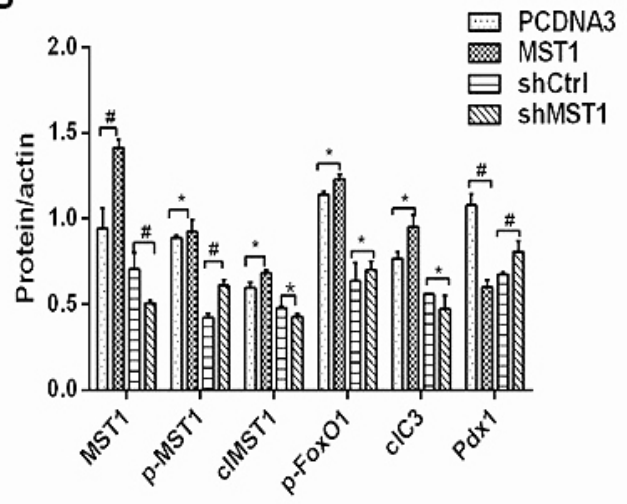
- 471 apoptotic signaling through phosphorylation at serine 82. *The Journal of biological*
472 *chemistry* 2010; 285: 6259-6264.
- 473 17. Lehtinen MK, Yuan Z, Boag PR, et al. A conserved MST-FOXO signaling pathway
474 mediates oxidative-stress responses and extends life span. *Cell* 2006; 125: 987-1001.
- 475 18. Liu P, Kao TP and Huang H. CDK1 promotes cell proliferation and survival via
476 phosphorylation and inhibition of FOXO1 transcription factor. *Oncogene* 2008; 27:
477 4733-4744.
- 478 19. Yuan Z, Lehtinen MK, Merlo P, et al. Regulation of neuronal cell death by MST1-
479 FOXO1 signaling. *The Journal of biological chemistry* 2009; 284: 11285-11292.
- 480 20. Valenti L, Rametta R, Dongiovanni P, et al. Increased expression and activity of the
481 transcription factor FOXO1 in nonalcoholic steatohepatitis. *Diabetes* 2008; 57: 1355-
482 1362.
- 483 21. Kitamura YI, Kitamura T, Kruse JP, et al. FoxO1 protects against pancreatic beta cell
484 failure through NeuroD and MafA induction. *Cell metabolism* 2005; 2: 153-163.
- 485 22. Wei B, Dui W, Liu D, et al. MST1, a key player, in enhancing fast skeletal muscle
486 atrophy. *BMC biology* 2013; 11: 12.
- 487 23. Jonsson J, Carlsson L, Edlund T, et al. Insulin-promoter-factor 1 is required for
488 pancreas development in mice. *Nature* 1994; 371: 606-609.
- 489 24. Johnson JD, Ahmed NT, Luciani DS, et al. Increased islet apoptosis in Pdx1^{+/-} mice.
490 *The Journal of clinical investigation* 2003; 111: 1147-1160.
- 491 25. Brissova M, Shiota M, Nicholson WE, et al. Reduction in pancreatic transcription
492 factor PDX-1 impairs glucose-stimulated insulin secretion. *The Journal of biological*
493 *chemistry* 2002; 277: 11225-11232.
- 494 26. Lv L, Chen H, Sun J, et al. PRMT1 promotes glucose toxicity-induced beta cell
495 dysfunction by regulating the nucleo-cytoplasmic trafficking of PDX-1 in a FOXO1-
496 dependent manner in INS-1 cells. *Endocrine* 2015; 49: 669-682.
- 497 27. Hennige AM, Ranta F, Heinzlmann I, et al. Overexpression of kinase-negative protein
498 kinase Cdelta in pancreatic beta-cells protects mice from diet-induced glucose
499 intolerance and beta-cell dysfunction. *Diabetes* 2010; 59: 119-127.
- 500 28. Dadi PK, Vierra NC, Ustione A, et al. Inhibition of pancreatic beta-cell
501 Ca²⁺/calmodulin-dependent protein kinase II reduces glucose-stimulated calcium
502 influx and insulin secretion, impairing glucose tolerance. *The Journal of biological*
503 *chemistry* 2014; 289: 12435-12445.
- 504 29. Chu ZLL, J. N, Al-Shamma, H.A., Jones, R.M. Combination therapy for the treatment
505 of diabetes and conditions related thereto and for the treatment of conditions
506 ameliorated by increasing a blood glp-1 level *International Patent Publication* 2009:
507 762-768.

- 508 30. Overton HA, Babbs AJ, Doel SM, et al. Deorphanization of a G protein-coupled
509 receptor for oleoylethanolamide and its use in the discovery of small-molecule
510 hypophagic agents. *Cell metabolism* 2006; 3: 167-175.
- 511 31. Flock G, Holland D, Seino Y, et al. GPR119 regulates murine glucose homeostasis
512 through incretin receptor-dependent and independent mechanisms. *Endocrinology*
513 2011; 152: 374-383.
- 514 32. Graves TK and Hinkle PM. Ca(2+)-induced Ca(2+) release in the pancreatic beta-cell:
515 direct evidence of endoplasmic reticulum Ca(2+) release. *Endocrinology* 2003; 144:
516 3565-3574.
- 517 33. Nakagawa T, Zhu H, Morishima N, et al. Caspase-12 mediates endoplasmic-reticulum-
518 specific apoptosis and cytotoxicity by amyloid-beta. *Nature* 2000; 403: 98-103.
- 519 34. Wellen KE and Hotamisligil GS. Inflammation, stress, and diabetes. *The Journal of*
520 *clinical investigation* 2005; 115: 1111-1119.
- 521 35. Yuan T, Lupse B, Maedler K, et al. mTORC2 Signaling: A Path for Pancreatic beta
522 Cell's Growth and Function. *J Mol Biol* 2018; 430: 904-918.
- 523 36. Ardestani A, Paroni F, Azizi Z, et al. MST1 is a key regulator of beta cell apoptosis
524 and dysfunction in diabetes. *Nat Med* 2014; 20: 385-397.
- 525 37. Guo H, He Y, Bu C, et al. Antitumor and apoptotic effects of 5-methoxypsoralen in
526 U87MG human glioma cells and its effect on cell cycle, autophagy and PI3K/Akt
527 signaling pathway. *Arch Med Sci* 2019; 15: 1530-1538.
- 528 38. Zhang Y, Zhang R and Ni H. Eriodictyol exerts potent anticancer activity against A549
529 human lung cancer cell line by inducing mitochondrial-mediated apoptosis, G2/M cell
530 cycle arrest and inhibition of m-TOR/PI3K/Akt signalling pathway. *Arch Med Sci*
531 2020; 16: 446-452.
- 532 39. Zhao M, Wang K, Shang J, et al. MiR-345-5p inhibits tumorigenesis of papillary
533 thyroid carcinoma by targeting SETD7. *Arch Med Sci* 2020; 16: 888-897.
- 534 40. Zhihong Z, Rubin C, Liping L, et al. MicroRNA-1179 regulates proliferation and
535 chemosensitivity of human ovarian cancer cells by targeting the PTEN-mediated
536 PI3K/AKT signaling pathway. *Arch Med Sci* 2020; 16: 907-914.
- 537 41. Eken MK, Ersoy GS, Kaygusuz EI, et al. Etanercept protects ovarian reserve against
538 ischemia/reperfusion injury in a rat model. *Arch Med Sci* 2019; 15: 1104-1112.

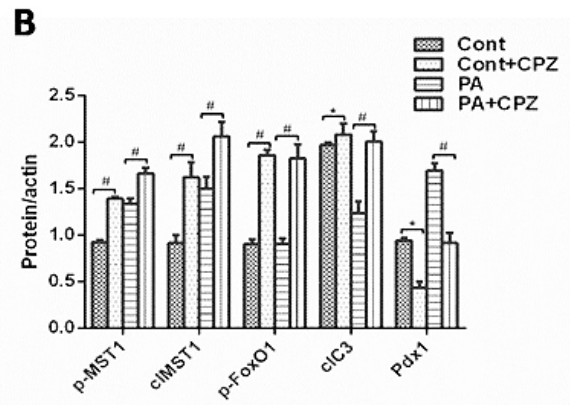
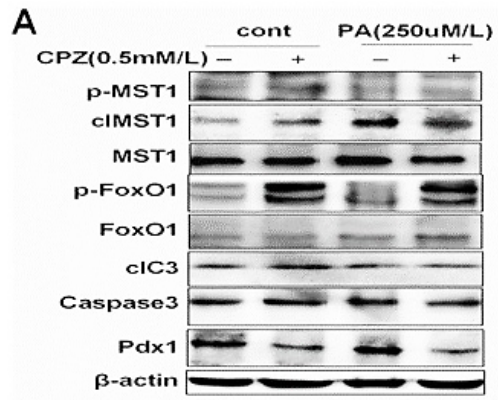
539



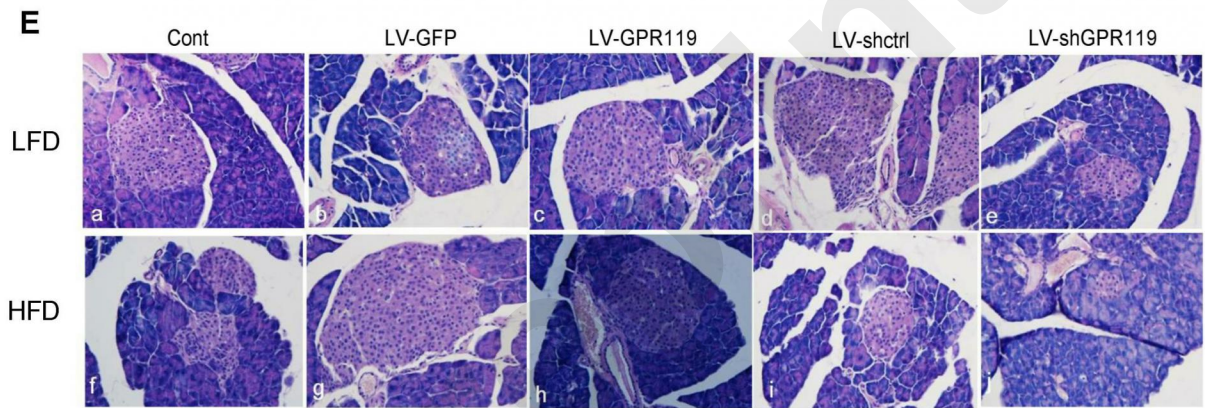
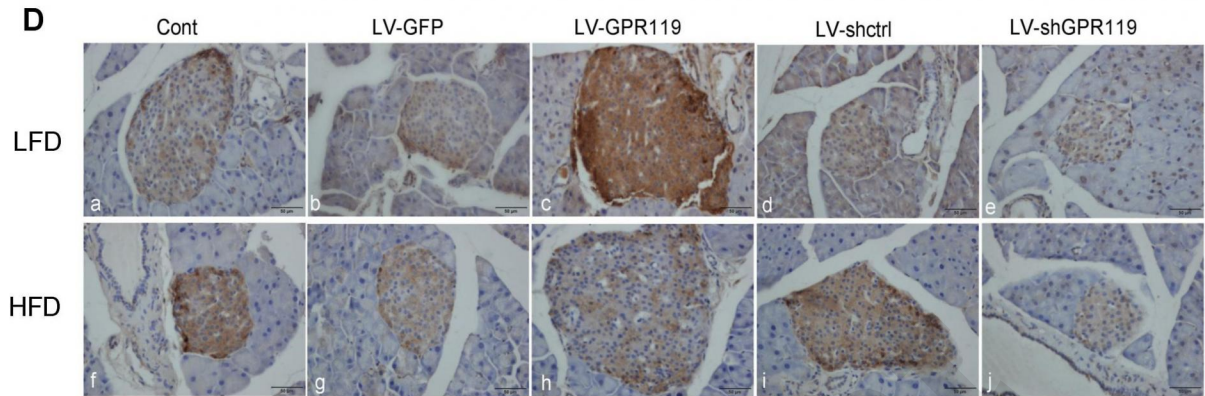
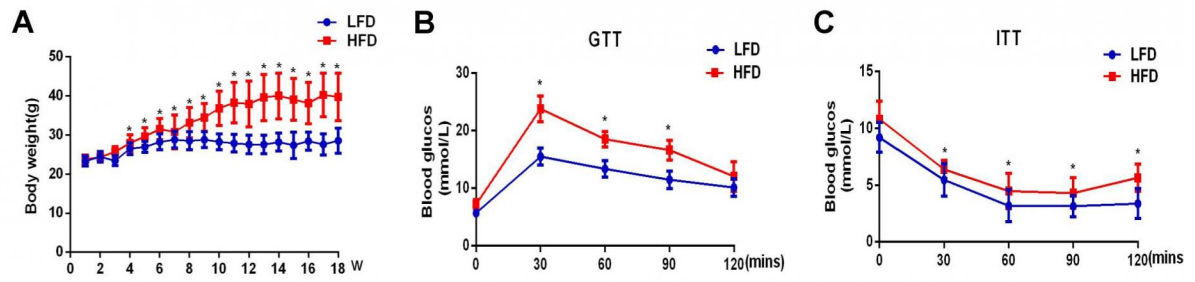
Preprint

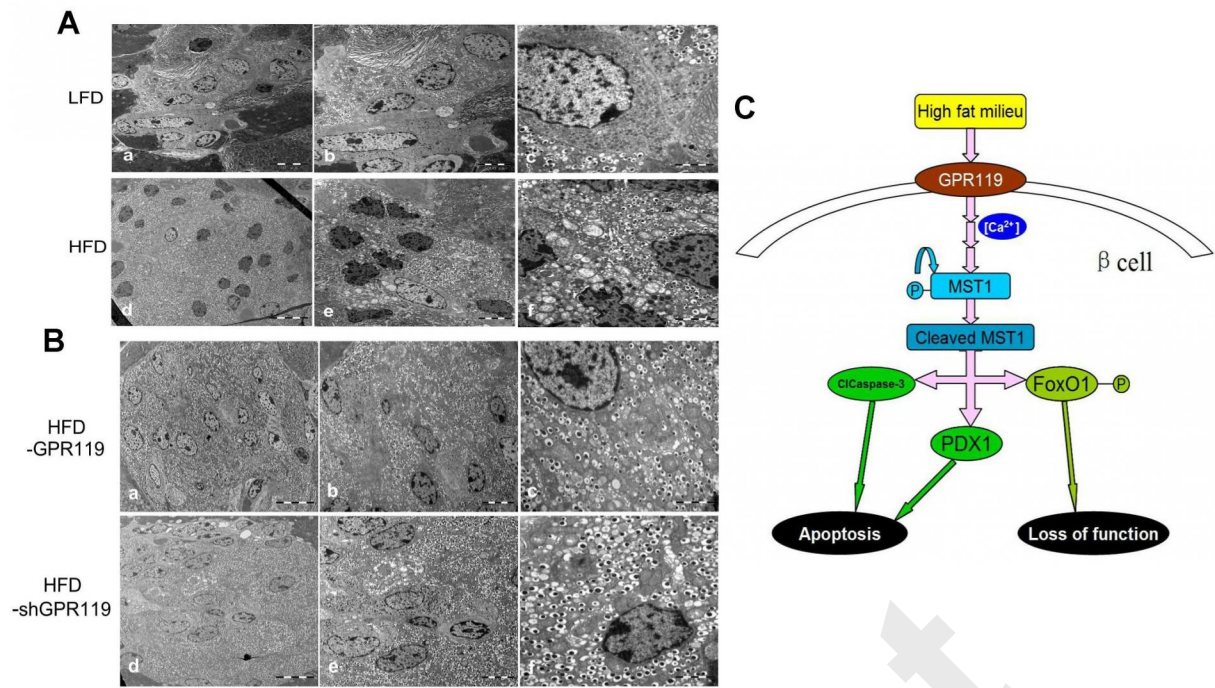
A**B**

Preprint

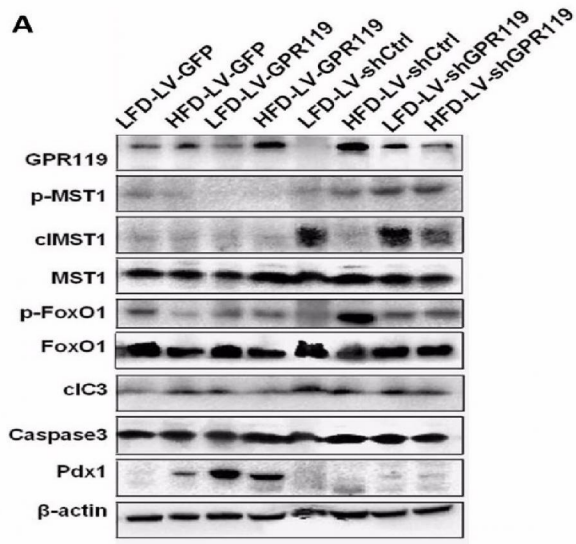
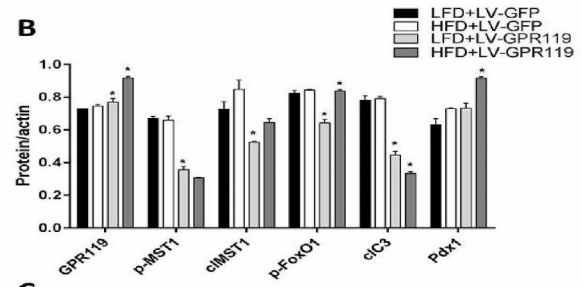
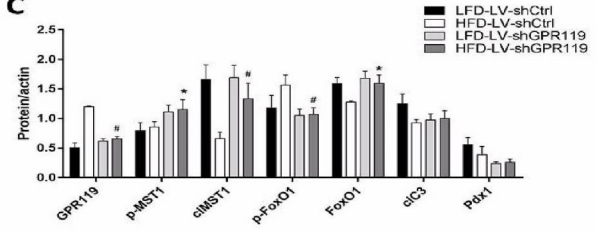


Preprint





Preprint

A**B****C**

Preprint